Clustering of Marine Bacteria in Seawater Enrichments

JAMES G. MITCHELL,* LYNETTE PEARSON, AND SIMON DILLON

Biological Sciences, Flinders University, Adelaide, SA 5001, Australia

Seawater enrichments of marine bacteria clustered in 20- to 50-μm-wide bands near air-water interfaces. The cells within the band travelled at up to 212 μm s^{-1} and at an average speed of 163 μm s^{-1}. Mean cell speeds peaked mid-run at 187 μm s^{-1}. At the end of the run, bacteria reversed direction rather than randomly reorienting. The duration of the stops during reversal was estimated at 18 ms, six to seven times shorter than that found in enteric bacteria. Cells hundreds of micrometers from the band travelled at half the speed of the bacteria in the band. The fastest isolate from the seawater enrichment was identified as *Shewanella putrefaciens* and had an average speed of 100 μm s^{-1} in culture. Air-water interfaces produced no clustering or speed changes in isolates derived from enrichments. Salinity and pH, however, both influenced speed. The speed and reversal times of the seawater enrichments indicate that the bacteria in them are better adapted for clustering around small point sources of nutrients than are either enteric or cultured marine bacteria.

Marine bacteria are thought to cluster around microscopic nutrient sources (7). If this occurs, the microscale complexity of at least some marine microbial communities is much greater than generally assumed (10). One consequence is that there may exist significant nutrient fluxes among microbes that go unmeasured in bulk water samples (5). Direct observational confirmation of this is precluded by the small size and low concentrations (cf. cultures) of marine bacteria, combined with the ubiquitous turbulence of the sea. As a result, research is inferential, based on models of motile bacteria (10), in vitro observation of chemotaxis (7), and unusual uptake kinetics (6). Models disagree over the generality of this clustering phenomenon and the ability of bacteria to respond to steep, short-lived chemical gradients (10, 16, 24). The research presented here used seawater enrichments to investigate the manner and speed with which marine bacteria responded to microscopic, narrow chemical gradients, similar to those that might be found in the pelagic environment.

Marine bacteria must overcome high rotational diffusion, shear from turbulence, and low nutrient concentrations to form clusters. These are added obstacles compared with classical systems, such as those in which *Proteus* cells aggregate on agar plates (15, 29), or the wide variety of bacteria that form bands in capillaries (1, 17, 18) or migrate in soil (21). To date, however, there is little work on the behavior of an individual cell in suspension, particularly around submillimeter point sources.

Analytical (24) and numerical (10) models indicate that the movement parameters used by enteric bacteria for taxis are far from optimal for responding to chemical gradients in the sea. Enteric bacteria move in discrete steps joined to form random walks (8). These walks are inefficient in the sense that the net speed up a chemical gradient is only a low percentage of the swimming speed. The bacteria have little alternative as Brownian motion reorients cells over a period of a few seconds (9). This situation is compounded outside of laboratory cultures by water movement.

Water movement in the ocean is turbulent. Bacterial speeds have been considered too low to counter the shear from oceanic turbulence (10, 24). Recent work, however, shows that marine bacteria in enriched seawater swim up to 10 times faster (19, 25) than enteric bacteria-based values used in ocean motility models (10, 16, 24).

The high speed, combined with the nanomolar nutrient concentrations of pelagic environments, makes motility much more energetically expensive for marine bacteria than for enteric bacteria (22, 25). These high speeds are not just a case of the marine bacteria directing more energy to their flagellar motors compared with enteric bacteria. Marine vibrios are known to possess sodium-pump flagellar motors as well as the proton-pump motors found in enteric bacteria (4). Motor differences apparently extend beyond the ion that is pumped. Fung and Berg (14) report that enteric motors fail before they reach the rotation rates found in marine bacteria (19). This indicates that motors driving some marine bacterial rotation are fundamentally distinct from those used by the enteric bacteria in their structure, as well as the ions used to drive them.

The discovery of rapid speed changes in marine bacteria suggests that their reaction times for sensing and responding could be much faster than the 0.2 s found in enteric bacteria (28). Mechanistically, this is not surprising as enteric responses are a factor of 10 slower than the theoretical limit for bacteria (28).

There may be selective pressure in the ocean for fast cells and rapid reactions because pelagic nutrient gradients emanate from small sources that are scoured by turbulence. The resulting shear erodes diffusive gradients around 10-μm phytoplankton to millimeter-sized particles (3, 11, 16) in tens to hundreds of seconds (24). In order for chemotaxis to function in such a system, the gradients must form on the order of tens of seconds (diffusive equivalent to hundreds of micrometers) with the bacteria responding on the same or a shorter time scale. The quicker the bacterial response is, the closer they will be able to remain near a nutrient source. Closeness minimizes exposure to shear and thus maximizes residence time in a high-nutrient environment. Here we build on previous work (25, 26) to examine how and how quickly marine bacteria respond in a heterogeneous chemical environment.

MATERIALS AND METHODS

Sampling and preparation. Bacterial communities from Brighton Beach seawater near Adelaide, South Australia, were used in all experiments. Tryptic soy broth was chosen as a nutrient source to increase cell number and stimulate

---

* Corresponding author. Mailing address: Biological Sciences, Flinders University, P.O. Box 2100, Adelaide, SA 5001, Australia. Electronic mail address: bijgm@cc.flinders.edu.au.

motility (25). Samples were incubated (20 to 23°C) for 15 h in 0.1% tryptic soy broth in sterile seawater. Aliquots of the enriched seawater were introduced into an optically flat slide chamber 7.5×10^{-3} cm deep and constructed according to the method of Mitchell et al. (25).

Microscopy. Cell speed was measured by dark-field microscopy on an Olympus BHT microscope at a magnification of ×200 with a halogen lamp set on maximum illumination. The combination of maximum illumination and dark-field microscopy ensured that cells down to 0.2 μm in diameter could be clearly viewed. Movement was recorded for approximately 1 min at 24 frames s^{-1} on a JVC TK-1280E video camera. The speeds of 10 cells from each recording were measured frame by frame. To induce clusters and high speeds, 0.3- to 1-mm-diameter air bubbles were introduced into the chamber. Cluster width was measured as the distance between the maximum slopes in cell density (25). Runs were defined as the distances between reversals. Angles between runs were measured as change from the line of movement of the first run to the line of movement of the second run.

Cluster isolates. High-speed cells were isolated from slides containing clusters and placed in a medium based on the work of Malmcrona-Friberg et al. (20) with the modification that the salts solution was replaced with artificial seawater. Identification was by classical and carbon utilization methods modified for marine bacteria (25).

Isolate manipulation. To determine whether the observed speeds and behavior were a result of external physical changes across the gradient, the influence of pH and salinity changes was examined. To starve cells, eight subcultures of the fastest pure marine bacterial isolate were grown in Marine Broth (Oxoid) overnight at 20°C and diluted 1:40 in vibrio artificial seawater, with or without a carbon source, modified from the work of Malmcrona-Friberg et al. (20, 25). Cultures were incubated at room temperature for 48 h. *Escherichia coli* cells were grown in nutrient broth overnight at 37°C. Both species were centrifuged at $600 \times g$ for 10 min. The resulting isolate pellets were resuspended in vibrio artificial seawater (no carbon) solutions with the pH previously adjusted to 6.2, 7.2, 8.2, and 9.2 with HCl and NaOH. For salinity experiments, the isolate was resuspended in vibrio artificial seawater (no carbon) solutions with sodium chloride concentrations of 2.0, 3.0, 4.0, and 5.0%. *E. coli* pellets were resuspended in phosphate chemotactic buffer (2) with pH values of 5.0, 6.0, 7.0, 8.0, and 9.0 or with sodium chloride concentrations of 2.0, 3.0, 4.0, and 5.0%.

Pattern assessment of bacterial runs. Standard descriptive statistics were not able to preserve, analyze, and display the behavioral pattern shown by the natural communities. To overcome this problem, phase diagrams were created by using sequential speed measurements of a single run as both the x and y values in a graph. This was done by using a chosen value as x and then the subsequent value in the series as y. More formally, the x and y coordinates were generated by applying the following equations: $(x_1 = s_1, y_1 = s_2), (x_2 = s_2, y_2 = s_3), \ldots, (x_n = s_n, y_n = s_{n+1})$, where s_n is the speed at position n in the run. The result is $n - 1$ pairs of x and y values. This is the spatial equivalent of taking an autocorrelation function of a time series with lag equal to 1.

RESULTS

Bacteria formed clusters with a mean width of 35 μm (± a 95% confidence interval of 4.1 μm). The length of the cluster along the bubble was determined by the size of the bubble. Individuals stayed within the cluster by changing direction at the end of each run (Fig. 1). Speeds were not uniform across the cluster line but ranged from 9 to 212 μm s^{-1}. The maximum speed occurred midrun (Fig. 2). Normalizing lengths of runs to between 0 and 1 for all cells and averaging the increments gave an arched speed pattern (Fig. 3). The mean maximum speed for an individual cell across a run was 187 (± 12) μm s^{-1}. Speeds varied between runs for the same individual. The fastest run for each individual in the community had a mean speed of 163 (± 24) μm s^{-1}. The mean speed around reversing was 47 (± 6.5) μm s^{-1}. Run lengths and times had means of 115 (± 33) μm and 1.04 (± 0.10) s for all runs of all individuals, respectively. The mean angle between runs was 171° (± 1.8°). This angle led us to term the direction change a reversal rather than a turn. Speed changes were most pronounced immediately before and after a reversal. Runs plotted as phase diagrams gave information on cell variability and behavior (Fig. 4 to 7).

For cells that remained outside the clusters, speeds ranged from 28 to 120 μm s^{-1}. The fastest cell had a mean maximum speed of 97 μm s^{-1} (± 2.8 μm s^{-1}). In 400 frames of analysis outside the cluster, there were no reversals by any bacteria, precluding measurement of run length and duration.
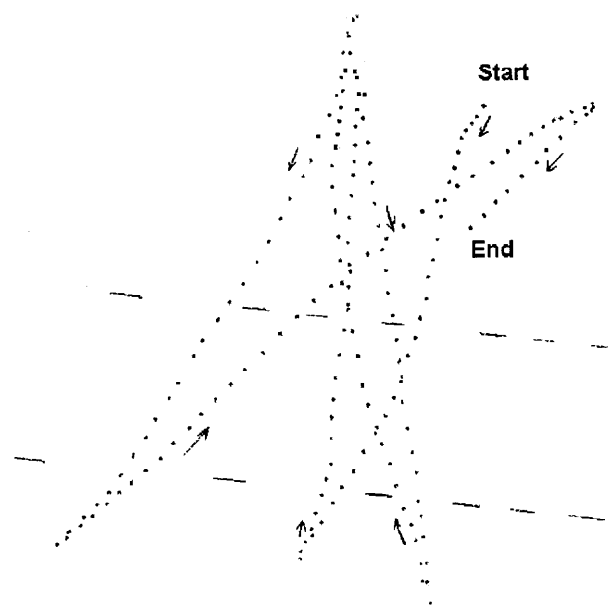

FIG. 1. A representative path of a marine bacterium from a natural community in a microcluster. Each irregular dot represents the cell position in a given frame. To avoid confusion among different paths near vertices, the dots were recorded in different colors (not shown). The dashed lines represent the edge of the cluster, defined as where the gradient in bacterial abundance is steepest as counted on freeze frames. Details of gradient assessment are provided by Mitchell et al. (25). Focusing on either the slide or the coverslip surface showed a high density of bacteria on the surface within the band compared with areas outside the band. The dashed lines are separated by 48 μm, the widest band measured. Extensions of the cell beyond the dashed lines are longer on the oxic than on the anoxic side. Many cells stayed within the band, but it was not possible to monitor them for more than a few frames. The figure is a scanned image of original data. The scanning process used to produce this figure resulted in loss of resolution. The general shape of the dots was not changed, but their relative size was enlarged by up to a factor of 2 to ensure visibility in the final publication.

A highly motile isolate with speeds closest to the natural community was identified as *Shewanella putrefaciens* by using Biolog (octal number, 0320-0000-0002-4404-1521-6777-1014-3420). Slides set up as with the natural communities produced speed and variation changes. At pH values of 6.2, 7.2, 8.2, and 9.2, the mean speeds were 72 (± 2.4), 76 (± 4.2), 100 (± 3.9), and 73 (± 2.9) μm s^{-1}, respectively. Salinity values of 20, 30,
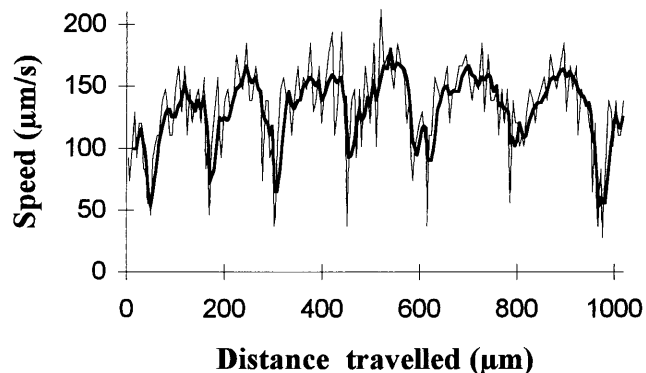

FIG. 2. The speed changes for a single representative cell from a natural community as a function of distance travelled. Each of the seven dips in the thin line below 65 μm s^{-1} represents a reverse. At no time did the apparent speed go to zero (see Discussion for explanation). The thin line represents the unsmoothed data. The thick line shows the results after applying a three-point running mean.
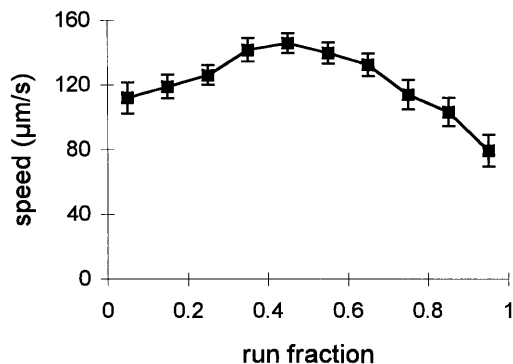
FIG. 3. The average speed during runs shows a maximum just before midrun. In order to compare runs of different lengths, runs were normalized between 0 and 1. The values were then grouped into bins that were 10% of the normalized run length, and points were plotted at the midbin interval. The error bars are the 95% confidence intervals.

40, and 50 ppt produced mean speeds of 127 ($\pm$ 2.4), 111 ($\pm$ 3.1), 105 ($\pm$ 4.0), and 97 ($\pm$ 3.0) μm s^{-1}. Phase diagrams were made of all manipulations (Fig. 5 and 6), and a random phase diagram was made for comparison (Fig. 7).

DISCUSSION

Some bacteria in seawater enrichments appear able to maintain position to approximately 1 run length (Fig. 1). These
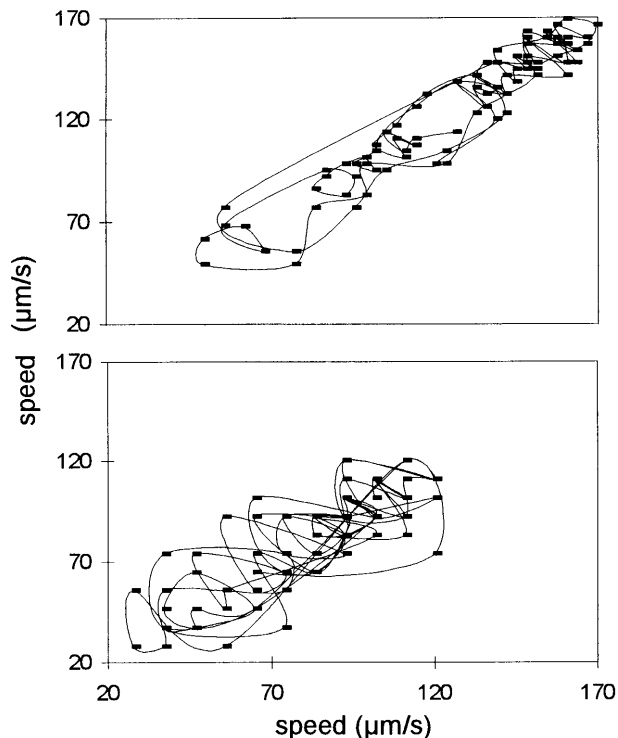

FIG. 4. Visualization of spatial autocorrelation (phase diagram) showing interframe speed changes for enriched seawater bacteria. Top, phase space for bacteria within the cluster. Bottom, the phase space for bacteria outside the cluster. The deviation from circularity indicates that the speed fluctuations and possibly the associated paths are not true random walks. Linear regression through the points gave a slope of 0.97 and an r^2 value of 0.89. Note that the points cluster into three groups. Lines join adjacent points. The farther apart two joined points are, the greater the speed change. Patterns held for all bacteria examined ($n = 26$).
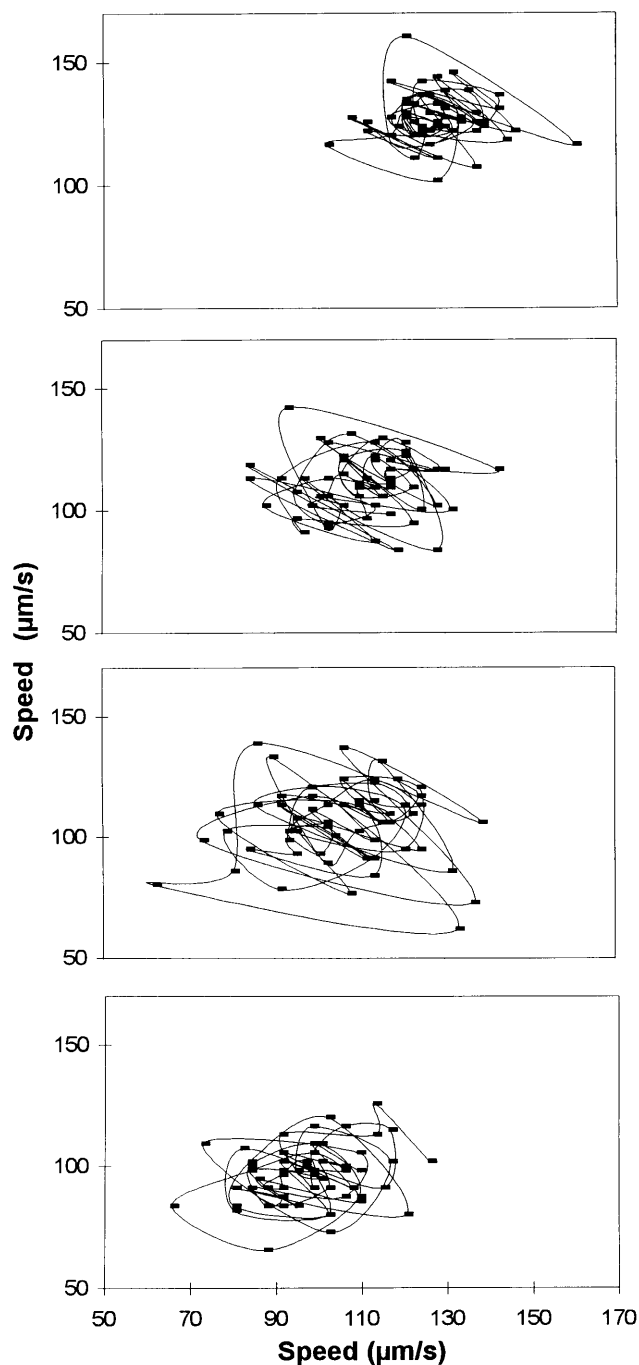

FIG. 5. Phase diagrams for *S. putrefaciens* isolated from the natural communities used in this work. The top graph represents bacteria at pH 6.2, and subsequent graphs, moving downward, are for pH values of 7.2, 8.2, and 9.2. The scales are the same for all axes. All r^2 values were <0.05.

bacteria possess high speed and rapid reversals. In this discussion, we explain how the rapid reversals cause a bacterium to remain in a circular area and how the high speed permits great sensitivity to chemical gradients. These two features combine to permit microscale clustering.

Direction reversals. Run reversals showed up as rapid decreases in speed that did not go to zero (Fig. 2). We interpret this to mean that reversals were significantly faster than the
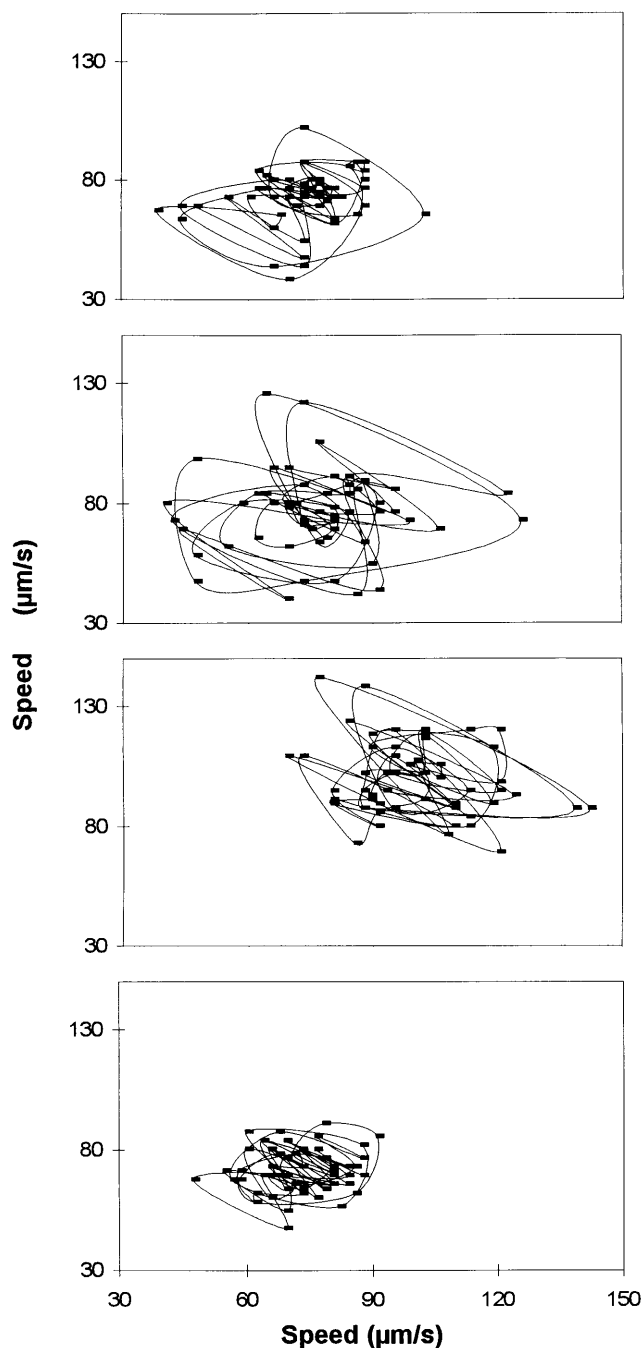
FIG. 6. Phase diagrams for *S. putrefaciens* isolated from the natural communities used in this work. The top graph represents bacteria at a salinity of 20 ppt, and subsequent graphs, moving downward, are for salinity values of 30, 40, and 50 ppt. The scales are the same for all axes. All r^2 values were <0.05.

FIG. 7. Reference phase diagrams of four bacterial tracks generated with Excel5 and the formula = RAND () $*$ 50 + 75 and plotted on the same scale range as in Fig. 5 and 6. All r^2 values were <0.05. RAND () $*$ 50 multiplies a random number by 50.

speed is 1/10 that of marine bacteria and reversal time has not been measured (23).

While 18 ms is fast compared with *E. coli*, it is well within the timeframe for a molecule to diffuse across a marine bacterium-sized cell. If molecular diffusivity inside the cell is assumed to be approximately 10^{-5} cm^2 s^{-1} and the cell diameter is 6 $\times$ 10^{-5} cm, then the mean time for a molecule to diffuse across a cell is on the order of 10^{-4} s, or about 2 orders of magnitude faster than the reversal time. If signal processing has all been done during the run, the difference must be due to flagellar motor switching mechanisms and flagellar bundle reassembly time.

Cluster formation and minimum width. Marine bacteria formed clusters approximately 1 run length wide (Fig. 1). This is at odds with the standard run-and-tumble model of bacterial movement, which requires multiple runs that result in imprecise positioning (9). We believe that the difference is due to the fast reactions described above and that no new mechanism is needed to explain our results. To support this position, we show that the principles described by Purcell (27) for the standard model explain the cluster width in a broad sense.

We begin by estimating the minimum length that a cell must travel to make one measurement. The length is $L = D/v$, where L is length, D is molecular diffusivity (10^{-5} cm^2 s^{-1}), and v is velocity (27). For the mean peak speed of 163 μm s^{-1}, the minimum length is 6 μm. Assuming that a decision can be made on two concentration measurements, the corresponding minimum bandwidth is 12 μm. This is less than our cluster width, but the cell does not always travel at the peak velocity, and so the required length will change over the course of the run. The minimum length, however, is short enough for the cell to make multiple measurements during the run and so rapidly detect the gradient edge. Rapid detection, combined with rapid reaction and the ability to reverse direction, permits the

frame rate (24 s^{-1}), since in no case did we see the speed drop to zero. A mean speed around reversals of 47 μm s^{-1} (Fig. 2 and Fig. 4 legend) suggests a reversal time of about 18 ms. This assumes that cells were travelling at 110 μm s^{-1} before stopping and that there was no inertia in starting or stopping (27). This is seven times faster than *E. coli* (8). However, *E. coli* tumbles rather than reverses. Bacterial isolates from lakes, such as *Chromatium minus*, do reverse direction, but their
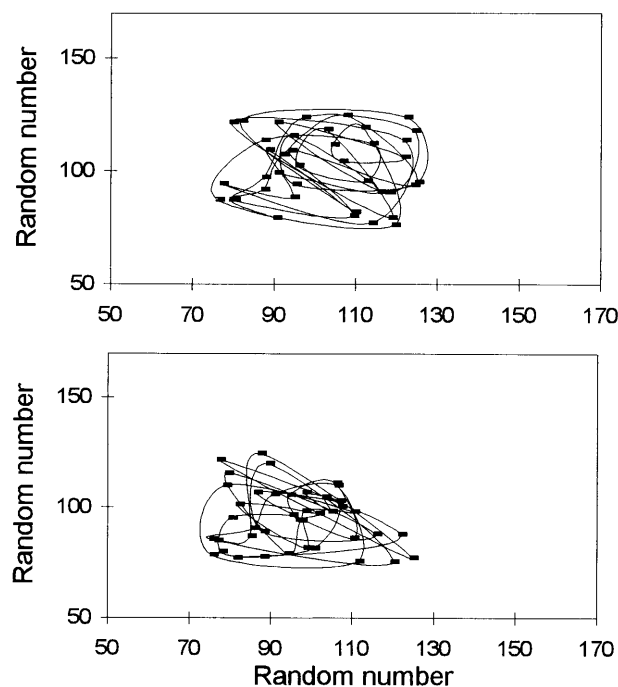
bacteria to stay in a small volume. If a number of bacteria have the same responses to the same parameters, this will result in a concentrated cluster of bacteria.

Residence time in the cluster. Reorientation of a cell due to Brownian motion and change in direction of flagellar rotation occurred during and at the end of runs (Fig. 1). Reversals, however, minimized the effect of reorientation and caused runs to rotate around a central axis area (Fig. 1). The mechanism of making continual rapid adjustments with reference to a sharp gradient suggests that cluster residence time in the sea may be limited not by motility parameters but by other factors such as the strength of the shear from turbulence and the depletion of signal. Previous work has assumed that motility would limit marine bacterial clustering ability (10), but these results and those of Fenchel (13) indicate that this is not necessarily so.

Whatever the mechanisms that permit and maintain the observed clusters, the potential ecological consequences are significant. Bacterioplankton that cluster closely enough to nutrient sources will maintain themselves in a diffusive core, away from turbulent shear that might carry them away from that source. Core size ranges from 45 to 450 μm (10) depending on shear intensity. The motility parameters described here would allow bacteria to remain in most diffusive cores in the ocean.

Error sources in the speed peak. While the reversal times were only inferred from our data, the speed during a run was measured directly. Figure 3 shows that the speeds were not constant over the run but peaked at midrun, with the beginning of the run starting at a higher speed than the end of the run. As described in our Materials and Methods here and in the work of Mitchell et al. (25), the resolution for fast bacteria is 9.2 μm s^{-1}. This makes speed measurements take on integer values of this resolution, effectively creating bins that only approximate the real speed. To compensate for binning of the speed measurements, values were averaged over each 10% of the run. Within each 10% fraction of the run, there were usually three points for each bacterial track. This reduced short-term variability. This smoothing process implicitly makes the assumption that binning of speed measurements increases the variability. Averaging speed measurements also minimizes the Brownian motion-driven component of the speed (26).

Phase diagrams. Unlike Fig. 3, the phase diagrams of Fig. 4 through 7 contain no averaging; they are the raw measurements. If Brownian motion is the predominant source of change in speed between increments, then all phase diagrams should resemble the graphs in Fig. 7, in which r^2 values are effectively 0. The top phase diagram r^2 value of 0.89 in Fig. 4 indicates that the contribution of Brownian motion to our measurements was a maximum of approximately 10%. This is an overestimate because it assumes that all unexplained variation in the graph is due to Brownian motion and not to variation within the speed control and energy production mechanisms of the cells.

The linearity of the phase diagrams in Fig. 4 indicates that adjacent speeds were similar. With the exception of the few long excursions in Fig. 4, which were associated with the reversals (Fig. 1 and 2), nonadjacent but nearby points were also grouped within the range of available speeds. The r^2 value of 0.42 outside the cluster compared with 0.89 inside the cluster indicates that the relationship is changeable in the natural community. This was not the case for the *S. putrefaciens* isolate (Fig. 5 and 6), for which the r^2 values explained less than 5% of the variation, similar to randomly generated sequences (Fig. 7). This indicates that speed variation in these figures is noise and that at least for this isolate there is no grouping of speed increments. Changes in salinity and pH did change speed and the amount of variation around that speed but did not repro-

duce the linear relation between speed at time t and at time t + 1 (Fig. 4). The clumping of points along the line indicates that some speeds and speed combinations occur more often than others. The cause of this could be multispeed motors or multiple types of motors. Atsumi et al. (4), for example, found multiple motor types and proposed that they were used at different viscosities. We propose the alternate hypothesis that the different motors are for different speeds.

Speed change. We observed very little or no futile switching, in which the cell stopped without reversing, as reported by Eisenbach et al. (12). To determine why will require future investigation of how tightly controlled switching mechanisms are and whether dual motor systems match each other's futile switching (4). The magnitude of the midrun acceleration was similar to the results of previous high-speed motility research, but the accelerations here appear to be a factor of 2 to 4 faster (26).

Motility in the pelagic environment. The ability to form narrow bands or clusters tens of micrometers wide and to move at high speeds is just what is required if bacteria are to cluster around nutrient-rich particles in a turbulent ocean. The model of Bowen et al. (10) assumed a maximum speed of 80 μm s^{-1}, no stopping time, and a reaction time, or response latency time, of 0.2 s. Doubling the speed and increasing the reaction time by a factor of 10 will increase clustering at the high shear found in the upper ocean. This is not to say that we suggest that free-living bacteria in the ocean are all clustering around particles as some models assume (16). The ability to form clusters must be reconciled with the results of Mitchell et al. (25), who showed that less than 10% of bacteria were motile in seawater at any one time but that >80% were capable of becoming motile after 10 to 12 h of exposure to nutrients. It is likely that bacterial clustering around nutrient sources, if it takes place, is an intermittent phenomenon that is a response by a subset of the community to discrete stimuli. In summary, bacteria with the behavior characteristics described here are capable of exploiting a particular niche in pelagic marine waters. Whether these gradients are most likely to occur naturally around phytoplankton, aggregates, decaying fecal pellets, or some other source of nutrients has yet to be determined. As the work with the isolate here has shown, for the time being motility parameters for clustering models are best obtained from seawater enrichments of marine bacteria.

REFERENCES

1. **Adler, J.** 1966. Chemotaxis in bacteria. Science **153:**708–716.
2. **Adler, J.** 1973. A method for measuring chemotaxis and use of the method to determine optimum conditions for chemotaxis by *Escherichia coli*. J. Gen. Microbiol. **74:**77–91.
3. **Alldredge, A. L., and Y. Cohen.** 1987. Can microscale chemical patches persist in the sea? Microelectrode study of marine snow, fecal pellets. Science **235:**689–691.
4. **Atsumi, T., L. McCarter, and Y. Imae.** 1992. Polar and lateral flagellar motors of marine Vibrio are driven by different ion-motive forces. Nature (London) **355:**182–184.
5. **Azam, F., and J. Ammerman.** 1984. Cycling of organic matter by bacterioplankton in pelagic marine ecosystems: microenvironmental considerations, p. 345–360. *In* M. J. R. Fasham (ed.), Flows of energy and materials in marine ecosystems. Plenum Press, New York.
6. **Azam, F., and R. E. Hodson.** 1981. Multiphasic kinetics for D-glucose uptake by assemblages of natural marine bacteria. Mar. Ecol. Prog. Ser. **6:**213–222.
7. **Bell, W., and R. Mitchell.** 1972. Chemotactic and growth responses of marine bacteria to algal extracellular products. Biol. Bull. **143:**265–277.

8. **Berg, H. C., and D. A. Brown.** 1972. Chemotaxis in *Escherichia coli* analysed by three-dimensional tracking. Nature (London) **239:**500–504.
9. **Berg, H. C., and E. M. Purcell.** 1977. Physics of chemoreceptors. Biophys. J. **20:**193–219.
10. **Bowen, J. D., K. D. Stolzenbach, and S. W. Chisholm.** 1993. Simulating bacterial clustering around phytoplankton cells in a turbulent ocean. Limnol. Oceanogr. **38:**36–51.
11. **Confer, D. R., and B. E. Logan.** 1991. Increased bacterial uptake of macromolecular substrates with fluid shear. Appl. Environ. Microbiol. **57:**3093–3100.
12. **Eisenbach, M., A. Wolf, M. Welch, R. R. Caplan, I. R. Lapidus, R. M. Macnab, H. Aloni, and O. Asher.** 1990. Pausing, switching and speed fluctuation of the bacterial flagellar motor and their relation to motility and chemotaxis. J. Mol. Biol. **211:**551–563.
13. **Fenchel, T.** 1994. Motility and chemosensory behaviour of the sulphur bacterium *Thiovulum majus*. Microbiology **140:**3109–3116.
14. **Fung, D. C., and H. C. Berg.** 1995. Powering the flagellar motor of *Escherichia coli* with external voltage source. Nature (London) **375:**809–812.
15. **Harshey, R. M.** 1994. Bees aren't the only ones: swarming in Gram-negative bacteria. Mol. Microbiol. **13:**389–394.
16. **Jackson, G. A.** 1989. Simulation of bacterial attraction and adhesion to falling particles. Limnol. Oceanogr. **34:**514–530.
17. **Liu, Z., and K. D. Papadapoulos.** 1995. Unidirectional motility of *Escherichia coli* in restrictive capillaries. Appl. Environ. Microbiol. **61:**3567–3572.
18. **Macnab, R. M.** 1987. Motility and chemotaxis, p. 732–759. *In* F. C. Neidhardt, J. L. Ingraham, K. B. Low, B. Magasanik, M. Schaechter, and H. E. Umbarger (ed.), *Escherichia coli* and *Salmonella typhimurium*: cellular and molecular biology, vol. 1. American Society for Microbiology, Washington, D.C.
19. **Magariyama, Y., S. Sugiyama, K. Muramoto, Y. Maekawa, I. Kawagishi, Y. Imae, and S. Kudo.** 1994. Very fast flagellar rotation. Nature (London) **371:**752.
20. **Malmcrona-Friberg, K., A. Goodman, and S. Kjelleberg.** 1990. Chemotactic responses of marine *Vibrio* sp. strain s14 (ccug15956) to low-molecular-weight substances under starvation and recovery conditions. Appl. Environ. Microbiol. **56:**3699–3704.
21. **McCaulou, D. R., R. C. Bales, and R. G. Arnold.** 1995. Effect of temperature-controlled motility on transport of bacteria and microspheres through saturated sediment. Water Resour. Res. **31:**271–280.
22. **Mitchell, J. G.** 1991. The influence of cell size on marine bacterial motility and energetics. Microb. Ecol. **22:**227–238.
23. **Mitchell, J. G., M.-R. Martinez-Alonso, J. Lalucat, I. Esteve, and S. Brown.** 1991. Velocity changes, long runs, and reversals in the *Chromatium minus* swimming response. J. Bacteriol. **173:**997–1003.
24. **Mitchell, J. G., A. Okubo, and J. A. Fuhrman.** 1985. Microzones surrounding phytoplankton form the basis for a stratified marine microbial ecosystem. Nature (London) **316:**58–59.
25. **Mitchell, J. G., L. Pearson, A. Bonazinga, S. Dillon, H. Khouri, and R. Paxinos.** 1995. Long lag times and high velocities in the motility of natural assemblages of marine bacteria. Appl. Environ. Microbiol. **61:**877–882.
26. **Mitchell, J. G., L. Pearson, S. Dillon, and K. Kantalis.** 1995. Natural assemblages of marine bacteria exhibiting high speed motility and large accelerations. Appl. Environ. Microbiol. **61:**4436–4440.
27. **Purcell, E.** 1977. Life at low Reynolds number. Am. J. Phys. **45:**3–10.
28. **Segall, J. E., M. D. Manson, and H. C. Berg.** 1982. Signal processing times in bacterial chemotaxis. Nature (London) **296:**855–857.
29. **Williams, F. D., and R. H. Schwarzhoff.** 1978. Nature of the swarming phenomenon in *Proteus*. Annu. Rev. Microbiol. **32:**101–122.